

## THERMAL CONDUCTIVITY OF INERT GASES AT LOW TEMPERATURES

A. G. Shashkov, N. A. Nesterov,  
V. M. Sudnik, and V. I. Aleinikova

UDC 533.27:536.23

An experimental and theoretical study of the thermal conductivity of helium, argon, and xenon is reported. The experimental apparatus is described, and the results are discussed.

There is increasing interest in the thermal conductivity of gases over broad temperature and pressure ranges.

The effort to intensify heat-exchange processes requires more accurate data on the thermal conductivity of gases for planning and designing various types of heat-exchange equipment, which is of fundamental importance in technological systems. This information is also of scientific interest, since it can assist in the development and refinement of transport theory and theoretical methods for calculating thermal conductivities.

The thermal conductivities of helium and argon at low temperatures have been studied more thoroughly; for xenon, on the other hand, very little information is available on the thermal conductivity at low temperatures and at atmospheric pressure, and the information which is available covers only the temperature range 194.65-273°K [1, 2].

### Experimental Apparatus

We used the absolute hot-filament method. The measuring cell used to study the thermal conductivity of gases over the temperature range 90-273.15°K is shown schematically in Fig. 1. Measuring tube 1 is made of type 365K molybdenum glass. Central heater 2, which doubles as a heat source and an internal resistance thermometer, is attached rigidly to light metal shell 8. This heater is stretched by a load of 4 g by means of spring 5, made of type A-1 tungsten wire, 50  $\mu$  in diameter. Resistance thermometer 3 is a double winding around the measuring tube. The use of this light shell, in which the measuring tube can be moved with respect to

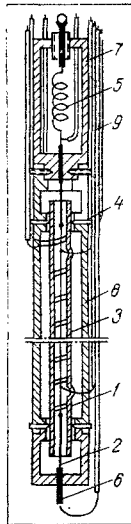


Fig. 1. Experimental cell. 1) Measuring tube; 2) internal resistance thermometer; 3) external resistance thermometer; 4) centering screws; 5) tungsten spring; 6) glass capillary; 7) metal frame; 8) metal shell; 9) insulating capillaries.

A. V. Lykov Institute of Heat and Mass Transfer, Academy of Sciences of the Belorussian SSR, Minsk. Translated from *Inzhenerno-Fizicheskii Zhurnal*, Vol. 30, No. 4, pp. 671-679, April, 1976. Original article submitted April 1, 1975.

*This material is protected by copyright registered in the name of Plenum Publishing Corporation, 227 West 17th Street, New York, N.Y. 10011. No part of this publication may be reproduced, stored in a retrieval system, or transmitted, in any form or by any means, electronic, mechanical, photocopying, microfilming, recording or otherwise, without written permission of the publisher. A copy of this article is available from the publisher for \$7.50.*

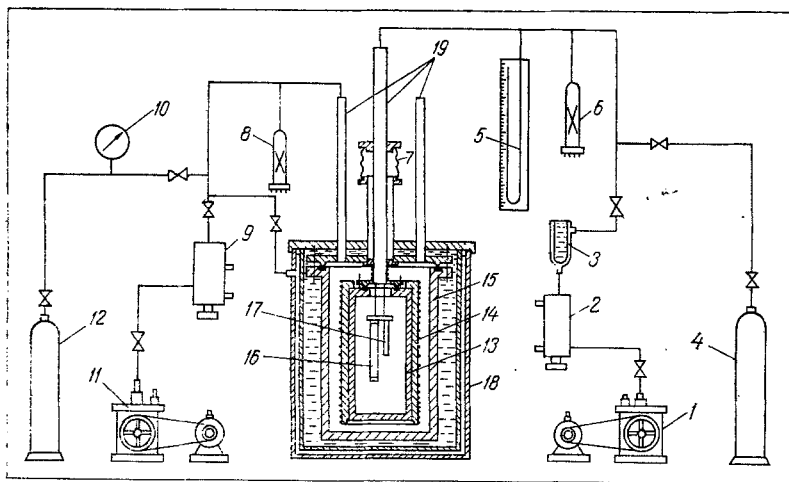


Fig. 2. Apparatus used to determine the thermal conductivity of gases at low temperatures. 1) VN-461M roughing pump; 2) TsVL-100 oil-vapor pump; 3) nitrogen cold trap; 4) gas tank; 5, 8) LT-2 pressure gauges; 6) mercury pressure gauge; 7) bellows; 9) N-2T oil-vapor pump; 10) vacuum gauge; 11) VN-2MG roughing pump; 12) tank with gaseous helium; 13) working chamber; 14) copper cylinder; 15) vacuum vessel; 16) measuring cell; 17) TSNP-1 low-temperature platinum resistance thermometer; 18) metal Dewar; 19) tubes for filling and evacuating the working chamber and the vacuum vessel, lines from measuring cell, and leads to the electric heaters and thermocouples.

the internal resistance thermometer (by means of eight centering screws 4), makes it possible to keep the eccentricity very low, within 0.01 mm, in a comparatively simple manner.

The resistance thermometers of the cell are made of type PL-1 platinum (All-Union State Standard 85-88-64) with a ratio  $R_{100}/R_0 = 1.3923$ , in accordance with the requirements imposed on platinum resistance thermometers [3]. These thermometers are calibrated on the basis of two reference points (the triple point of water [4] and the boiling point of water [5]) and against a type TSPN-1 low-temperature platinum resistance thermometer (at  $-182.99^\circ\text{C}$ ). The ratios of the resistances at 100 and  $0^\circ\text{C}$  for the internal and external are 1.3887 and 1.3889, respectively.

The geometric dimensions of the measuring cell and the calibration data on the resistance thermometers are as follows: the diameter of the platinum wire of the heater is 0.1 mm; the inside diameter of the measuring tube is 3.508 mm; the outside diameter of the measuring tube is 5.467 mm; the length of the measuring region is 99.898 mm; the thickness of the layer of test material is 1.704 mm; the eccentricity of the wire heater with respect to the axis of the tube is 0.01 mm; the resistance of the internal thermometer at  $0^\circ\text{C}$  is  $1.270 \Omega$ ; the temperature coefficient of the internal thermometer is  $3.8873 \cdot 10^{-3}$ ; the resistance of the external thermometer at  $0^\circ\text{C}$  is  $7.0712 \Omega$ ; the temperature coefficient of the external thermometer is  $3.8891 \cdot 10^{-3}$ ; the resistance of the internal thermometer at  $-182.99^\circ\text{C}$  is  $0.31201 \Omega$ ; the resistance of the external thermometer at  $-182.99^\circ\text{C}$  is  $1.73595 \Omega$ ; the constant A, calculated from the geometric dimensions, is 5.672; the constant B, calculated from the geometric dimensions, is  $0.7088/\lambda_{\text{wa}}$ .

The measuring tube is calibrated and the geometric dimensions of the resistance thermometers and the eccentricity are determined with a binocular toolmaker's microscope within  $\pm 0.002 \text{ mm}$ .

Figure 2 shows the experimental apparatus used to determine the thermal conductivity of the gases at low temperatures.

In the working chamber of the cryostat 13, which rests on a cold base in copper cylinder 14, is the measuring cell 16 and the TSNP-1 low-temperature platinum resistance thermometer. On the lateral surface of the copper cylinder are three independent (separate) double-

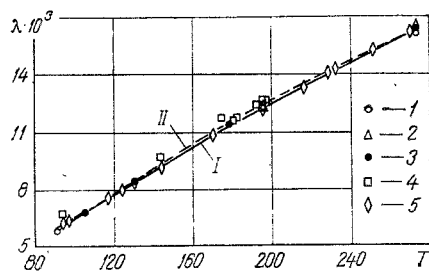


Fig. 3

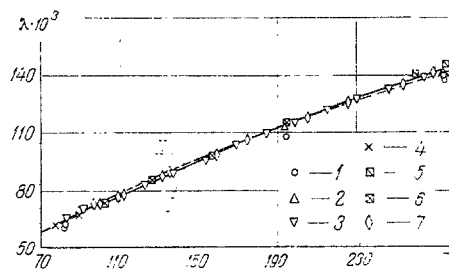


Fig. 4

Fig. 3. Thermal conductivity of gaseous argon as a function of the temperature at atmospheric pressure. I) Recommended values from [17]; II) smoothed recommended values from [16]; 1) experimental data of [10]; 2) [1]; 3) [2]; 4) [11]; 5) experimental data of pressure study. Here  $\lambda$  is in W/m·deg and T is in °K.

Fig. 4. Thermal conductivity of gaseous helium as a function of the temperature at atmospheric pressure. I) Recommended values from [17]; II) smoothed recommended values from [16]; 1) experimental data of [10]; 2) [1]; 3) [12]; 4) [13]; 5) [14]; 6) [15]; 7) experimental data of present study.

wound heating windings (upper, central, and lower windings). These windings are made of Constantan wire 0.5 mm in diameter. The upper winding is connected in series with a heater which is double-wound on tube 19. This heater heats the cap of the working chamber and is used to offset the heat loss. The working chamber is placed in a hollow metal vacuum vessel 15.

Before an experiment, the working chamber and vessel 15 are evacuated and filled with the test gas and the heat-exchange gas (helium), respectively. After the working chamber is cooled in the Dewar with liquid nitrogen, 18, to the required temperature, the heat-exchange gas is evacuated. The temperature is brought to the set value and held there by an automatic regulation system, consisting of three absolute copper-Constantan thermocouples, placed at the center of each heater; a pulse generator; a stepping switch; a temperature controller (an R-306 potentiometer); an Fl15-VI photoamplifier; a UE-109 electronic amplifier; and an RD-09 reversible motor, which connects the heaters to, and disconnects them from, a regulated ac power supply by means of a relay system.

The copper-Constantan differential thermocouples are used to monitor the uniformity of the temperature field along the height of the working chamber. During the experiments, the temperature drop between the center of the lower part of the working chamber and the center of the upper part is less than 0.05-0.1°C.

Hermetically sealed connectors in tubes 19 are provided for the gas and vacuum lines running from the measurement cell to the measuring system, the leads to the power supplies for the electric heaters, and the leads to the regulating and control thermocouples.

The voltage drop across the thermometers is measured with a potentiometer; the drop across the external resistance thermometer is measured with an R-306 potentiometer, and that across the internal thermometer is measured with R-300 and R-307 potentiometers. When a steady state was reached (this took no longer than 4 h), the voltage drop across the thermometers was measured at least 10 times with the current flowing in the opposite directions, and the results were averaged.

This apparatus can also be used to study the thermal conductivity of mixtures of gases, since the volume of the working chamber (13) (Fig. 2) is about 10 times the volume at room temperature, so that thermodiffusion can be eliminated [6].

### Experimental Results

In the hot-filament method, the thermal conductivity can be determined from

$$\lambda = \frac{AQ_{\tau}}{\Delta T_{msr} - BQ_{\tau} \pm \Delta T_{cali}}, \quad \text{where} \quad A = \frac{\ln \frac{d_2}{d_1}}{2\pi l}, \quad B = \frac{\ln \frac{d_3}{d_2}}{2\pi l \lambda_{wa}};$$

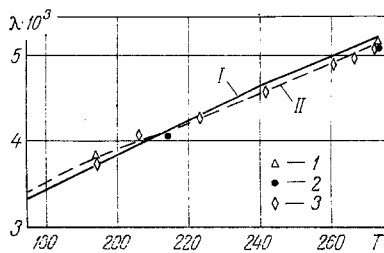


Fig. 5. Thermal conductivity of gaseous xenon as a function of the temperature at atmospheric pressure. I) Recommended values from [17]; II) smoothed recommended values from [16]; 1) experimental data of [1]; 2) [2]; 3) experimental data of present study.

$d_1$ ,  $d_2$ , and  $d_3$  are the diameter of the platinum-heater wire, the inside diameter of the glass measuring tube, and the outside diameter of this tube;  $l$  is the length of the measuring region;  $Q_T$  is the heat which is transferred by conduction through the layer of test material in the measuring region;  $\Delta T_{msr} = T_1 - T_2$  is the difference between the indications of the internal and external resistance thermometers;  $\Delta T_{cali}$  is the calibration correction to the indications of the internal thermometer on the basis of the external thermometer;  $\lambda_{wa}$  is the thermal conductivity of the wall of the measuring tube; and  $BQ_T = \Delta T_{wa}$  is the temperature drop in the wall of the measuring tube. In analyzing the experimental data we took into account the temperature dependence of the thermal conductivity of glass on the basis of [7].

In the experiments we used highly pure helium (99.985%) the argon was 99.987% pure, and the xenon was 99.9% pure.

The operation of the apparatus was tested on the basis of a well-studied gas: argon. The data obtained on the thermal conductivity of argon (Fig. 3) turn out to agree well with the most reliable experimental data in the literature [1, 2, 8-11]. The maximum discrepancy between our results and these results from the literature is within 1%; the data of [11] are slightly higher.

Figure 4 and 5 show our experimental results and those obtained by other investigators for helium and xenon. For helium, our results agree well with the experimental data of [1, 11, 12-15]; the maximum discrepancy at any point is 1.5%. In terms of the thermal conductivity of xenon (Fig. 5), our data agree better with the data of [2] and are approximately equal to the results in [16]. The high values of the data in [1] are apparently due to the error in the determination of the sum of the corrections for radiation and heat loss from the ends of the heater at the high value of this correction [17].

In calculating the thermal conductivity we took into account the heat loss along the electrical leads and the correction for radiative heat transfer.

The corrections to the indications of the internal thermometer on the basis of the external thermometer and the TSNP-1 platinum resistance thermometer at currents too low to cause heating were checked before each measurement ( $\Delta T_{cali}$ ). The corrections for the temperature drop, the eccentricity, and the change in the geometric dimensions of the cell as a function of the temperature were also found by measurements and calculations. All these corrections turned out to lie within the experimental error and were thus ignored.

With the particular geometric dimensions of this measuring tube, there is no convection, since the product of the Gr and Pr numbers in these experiments was less than 1000,

Table 1 shows the experimental results for helium, argon, and xenon. Here  $T_1$  and  $T_2$  are the indications of the internal and external resistance thermometers,  $Q$  is the total heat evolution of the heater,  $Q_r$  is the heat transferred by radiation from the heater to the wall of the measuring tube,  $Q_k$  is the heat transferred along the current and potential leads,  $\lambda$  is the thermal conductivity of the test substance,  $T_{me}$  is the temperature of the test substance, and  $\Delta T$  is the temperature drop in the layer of test material.

The error in our data was evaluated on the basis of the standard substance - argon [17] - by the method of [19].

Table 1 compares our results with the recommended tabulated values from [17]. The maximum deviation of our values for the thermal conductivity of argon from the tabulated values reaches 1.2% at certain points. At a fiducial probability of 0.95, the experimental error is  $\pm 0.5\%$ .

TABLE 1. Experimental Data for Determining the Thermal Conductivity

$T_1, K$	$T_2, K$	$Q \cdot 10^3, W$	$Q_T \cdot 10^3, W$	$Q_K \cdot 10^3, W$	$\frac{Q_K}{Q}, \%$	$Q_T \cdot 10^3, W$	$T_{me}, K$	$\frac{\lambda \cdot 10^3}{W}, m \cdot deg$	$\Delta T, K$
Helium									
91,96	91,03	1146,8	0,001	9,1	0,79	1137,7	91,50	70,91	0,91
92,98	91,33	2032,2	0,018	16,4	0,81	2015,8	92,16	71,01	1,61
98,05	96,37	2128,2	0,022	15,5	0,73	2112,7	97,21	73,06	1,64
99,30	97,25	2608,7	0,028	20,1	0,77	2588,6	98,28	73,41	2,00
100,99	99,49	1935,1	0,023	15,0	0,78	1920,1	100,24	74,08	1,47
111,21	108,87	3167,4	0,025	23,2	0,73	3144,2	110,04	77,87	2,29
113,97	110,49	4834,2	0,088	35,4	0,73	4798,7	112,23	79,81	3,41
134,49	129,39	7763,1	0,26	53,5	0,69	7709,3	131,94	87,63	4,99
137,90	134,04	6074,9	0,22	41,4	0,68	6033,3	135,97	90,53	3,78
163,43	156,14	12600,0	0,84	81,8	0,65	12517,4	159,79	99,43	7,14
178,78	171,41	13650,7	0,64	84,9	0,62	13565,2	175,10	106,60	7,22
211,24	201,10	20932,9	3,5	125,4	0,60	20804,0	206,17	118,80	9,93
231,86	222,36	20929,8	4,8	121,5	0,58	20803,5	227,11	126,87	9,30
259,90	247,51	29264,9	9,96	166,1	0,57	29088,8	253,71	136,24	12,11
279,04	269,33	24122,5	105,0	132,9	0,55	23884,6	274,19	142,75	9,49
Argon									
96,11	91,06	574,8	0,06	22,6	3,93	552,1	93,59	6,21	5,07
97,77	94,72	355,1	0,38	9,1	2,56	345,6	96,25	6,45	3,04
123,38	111,49	1622,6	0,38	36,7	2,26	1585,5	117,44	7,58	11,84
124,97	121,42	510,3	0,33	11,4	2,23	498,6	123,20	7,99	3,56
131,63	126,01	819,9	0,26	1,9	2,32	817,7	128,82	8,27	5,64
145,89	140,86	831,6	0,36	17,6	2,12	813,6	143,38	9,19	5,01
171,10	168,93	420,7	0,32	8,1	1,93	412,3	170,02	10,78	2,12
199,36	188,82	2296,0	2,8	43,1	1,88	2250,1	194,09	12,14	10,57
218,65	211,88	1617,9	2,7	28,0	1,73	1587,2	215,27	13,34	6,71
231,67	224,78	1719,4	3,5	29,1	1,69	1686,8	228,23	13,93	6,85
237,56	226,42	2857,5	6,2	49,9	1,75	2801,4	231,99	14,30	11,11
256,71	246,44	2799,1	7,9	48,7	1,74	2742,5	251,58	15,19	10,24
276,51	266,23	2994,3	10,6	47,9	1,60	2935,8	271,37	16,24	10,25
Xenon									
202,51	186,91	1067,1	4,3	36,5	3,42	1026,3	194,71	3,73	15,59
209,19	202,54	493,7	2,2	16,1	3,26	475,4	205,87	4,05	6,65
226,43	218,63	606,0	3,6	19,2	3,17	583,2	222,53	4,25	7,79
247,48	235,37	1012,8	8,0	32,4	3,20	972,4	241,43	4,56	12,10
271,39	249,67	1952,4	19,8	60,4	3,09	1872,2	260,53	4,89	21,70
276,21	255,53	1885,2	19,7	57,3	3,04	1808,2	265,87	4,96	20,66
282,29	260,83	2008,4	22,6	60,9	3,03	1924,9	271,56	5,09	21,44

TABLE 2. Experimental and Calculated Data on the Thermal Conductivity of Helium

$T, K$	$\lambda_{exp} \cdot 10^3$	L-J [20]		exp-6 [21]		Morse [23]	
		$\lambda_{calc} \cdot 10^3$	$\Delta$	$\lambda_{calc} \cdot 10^3$	$\Delta$	$\lambda_{calc} \cdot 10^3$	$\Delta$
91,50	70,91	71,542	+0,88	67,254	-5,4	68,425	-3,6
92,16	71,01	71,885	+1,2	67,589	-5,1	68,737	-3,3
97,21	73,06	74,433	+1,8	70,094	-4,2	71,066	-2,8
98,28	73,41	74,962	+2,1	70,616	-4,0	71,547	-2,6
100,24	74,08	75,946	+2,5	71,589	-3,5	72,441	-2,4
110,04	77,87	80,672	+3,5	76,444	-1,9	76,895	-1,3
112,23	79,81	81,712	+2,3	77,478	-3,0	77,882	-2,5
131,94	87,63	90,809	+3,5	86,678	-1,1	86,719	-1,05
135,97	90,53	92,599	+2,2	88,485	-2,3	88,527	-2,3
159,79	99,43	102,83	+3,3	98,97	-0,46	99,212	-0,22
175,10	106,60	109,1	+2,3	105,47	-1,1	105,85	-0,71
206,17	118,80	121,26	+2,0	117,98	-0,7	117,33	-1,3
227,11	126,87	128,97	+1,6	126,29	-0,46	124,97	-1,5
253,71	136,24	138,66	+1,7	136,26	+0,02	134,62	-1,2
274,19	142,75	145,71	+2,0	143,9	+0,8	142,03	-0,51

Note. In Tables 2-4,  $\lambda$  is expressed in W/m·deg;  $\Delta = (\lambda_{calc} - \lambda_{exp})/\lambda_{calc}, \%$ .

TABLE 3. Experimental and Calculated Data on the Thermal Conductivity of Argon

T, K	$\lambda_{\text{exp}} \cdot 10^3$	L-J [20]		exp-6 [21]		Morse [23]	
		$\lambda_{\text{calc}} \cdot 10^3$	$\Delta$	$\lambda_{\text{calc}} \cdot 10^3$	$\Delta$	$\lambda_{\text{calc}} \cdot 10^3$	$\Delta$
93,59	6,21	5,949	-4,4	5,919	-4,9	5,912	-5,0
96,25	6,45	6,075	-6,2	6,091	-5,9	6,079	-6,1
117,44	7,58	7,452	-1,7	7,454	-1,7	7,583	+0,04
123,20	7,99	7,831	-2,0	7,832	-2,0	7,942	-0,6
128,82	8,27	8,173	-1,2	8,166	-1,3	8,217	-0,65
143,38	9,19	9,093	-1,1	9,083	-1,2	8,944	-2,8
170,02	10,78	10,738	-0,39	10,717	-0,59	10,340	-4,3
194,09	12,14	12,147	+0,06	12,121	-0,16	11,694	-3,8
215,27	13,34	13,341	+0,007	13,311	-0,22	12,995	-2,4
228,23	13,93	14,052	+0,87	14,019	+0,63	13,844	-0,62
231,99	14,30	14,250	-0,35	14,218	-0,58	14,10	-1,4
251,58	15,19	15,287	+0,63	15,251	+0,4	15,145	-0,3
271,37	16,24	16,233	-0,04	16,205	-0,22	15,960	-1,8

TABLE 4. Experimental and Calculated Data on the Thermal Conductivity of Xenon

T, K	$\lambda_{\text{exp}} \cdot 10^3$	L-J [20]		L-J [21]		exp-6 [21]	
		$\lambda_{\text{calc}} \cdot 10^3$	$\Delta$	$\lambda_{\text{calc}} \cdot 10^3$	$\Delta$	$\lambda_{\text{calc}} \cdot 10^3$	$\Delta$
194,71	3,73	3,553	-5,0	3,583	-4,1	3,617	-3,1
205,87	4,05	3,766	-7,5	3,800	-6,6	3,829	-5,8
222,53	4,25	4,075	-4,3	4,113	-3,3	4,137	-2,7
241,43	4,56	4,415	-3,3	4,471	-2,0	4,490	-1,6
260,53	4,89	4,763	-2,7	4,830	-1,2	4,847	-0,89
265,87	4,96	4,863	-2,0	4,924	-0,73	4,939	-0,44
271,56	5,09	4,973	-2,4	5,025	-1,3	5,038	-1,0

We also compared our experimental data with the corresponding theoretical values of  $\lambda$  calculated on the basis of the rigorous Chapman-Enskog molecular-kinetics theory [20].

The calculation was carried out for several potentials: the Lennard-Jones (6-12) potential [20-22], a modified Buckingham (exp-6) potential [21, 22], and a Morse potential [23, 24]. The parameters of the intermolecular potential functions  $\epsilon$  and  $\sigma$  given in [20-22, 24] were determined from experimental data on the viscosity; in [23] they were determined on the basis of the second virial coefficient.

The calculated results are shown in Tables 2-4.

For helium, the experimental data can be described well by a Lennard-Jones potential with the parameters  $\epsilon/k = 10.22$  K and  $\sigma = 2.576$  Å [20] and by a Morse potential with  $\epsilon/k = 8.55$  K,  $\sigma = 3.687$  Å, and  $c = 6.0$  [23]. The Lennard-Jones potential overestimates the thermal conductivity, while the Morse potential underestimates it. The maximum discrepancy is 3.6%. For the modified Buckingham potential with  $\epsilon/k = 9.16$  K,  $\sigma = 3.135$  Å, and  $\alpha = 12.4$  [21], the maximum discrepancy between the calculated and experimental values of  $\lambda$  is 5.4%.

For argon, the experimental data are described best by the values calculated on the basis of the Lennard-Jones potential with  $\epsilon/k = 124.0$  K and  $\sigma = 3.418$  Å [20] and the Buckingham potential with  $\epsilon/k = 123.2$  K,  $\sigma = 3.866$  Å, and  $\alpha = 14.0$  [21].

A significant discrepancy between the calculated and experimental values (about 6%) is observed at the lowest temperatures; elsewhere the discrepancy is less than 2%.

For xenon, the theoretical values of the thermal conductivity calculated on the basis of the Lennard-Jones potential with  $\epsilon/k = 256$  K and  $\sigma = 3.92$  Å [21] and the exp-6 potential with  $\epsilon/k = 260$  K,  $\sigma = 4.40$  Å, and  $\alpha = 14.8$  [21] show a maximum discrepancy on the order of 6% at temperatures in the range 194.71-222.53°K; elsewhere the discrepancy is less than 2%.

As was shown in [18], the quantum corrections for inert gases are important only for helium over the temperature range 4-20°K; these corrections were accordingly ignored in the present study.

## LITERATURE CITED

1. W. Kannulik and E. Carman, Proc. Phys. Soc., 65B, 701 (1952).
2. F. G. Keyes, Trans. ASME, 76, 809 (1954).
3. M. M. Popov, Thermometry and Calorimetry [in Russian], Izd. MGU, Moscow (1954).
4. F. Z. Alieva, Tr. Vses. Nauchno-Issled. Inst. Metrolog., No. 35(95), 5 (1958).
5. F. Z. Alieva and V. P. Chekulaev, Tr. Inst. KSIP, No. 51(III), 35 (1961)
6. I. A. Kulakov, Izv. Voronezh. Gos. Pedinst., No. 17, 85 (1955).
7. N. V. Tsederberg, Thermal Conductivities of Gases and Liquids [in Russian], GÉI (1963).
8. W. Schwarze, Phys. Z., 4, 229 (1903).
9. A. Michels, J. V. Sengers, and L. M. M. Van de Klundert, Physica, 29, 149 (1963).
10. A. Eucken, Phys. Z., 14, 324 (1913).
11. A. Ziebleand and J. Burton, Brit. J. Appl. Phys., 9, 52 (1958).
12. A. L. Johnston and E. R. Grilly, J. Chem. Phys., 14, 233 (1946).
13. J. B. Ubbink and W. J. de-Haas, Physica S'Crav, 10, 465 (1943).
14. P. Mukhopadhyay and A. K. Barua, Brit. J. Appl. Phys., 18, 635-640 (1967).
15. I. F. Golubev and I. B. Shpagina, Gazovaya Prom-st', 8, 40 (1966).
16. Thermophysical Properties Research Center, Standard Reference Data on the Conductivity of Selected Materials, Part 3 (1968), pp. 338-340. Final Report on NBS-NSRDS, Contract CST-1346.
17. N. B. Vargaftik, L. P. Filippov, N. A. Tarzimanov, and R. P. Yurchak, Thermal Conductivities of Gases and Liquids (Handbook Data) [in Russian], Izd. KSMiIP pri SM SSSR (1970).
18. V. S. Yargin and G. I. Belashova, Inzh.-Fiz. Zh., 27, No. 6 (1974).
19. O. A. Sergeev, Fundamental Metrology of Thermophysical Measurements [in Russian], Izd. Standartov, Moscow (1972).
20. J. O. Hirschfelder, C. F. Curtiss, and R. B. Bird, Molecular Theory of Gases and Liquids, Wiley, New York (1954).
21. W. Hogervorst, Physica, 51, No. 1 (90 103) (1971).
22. Zà Kestin, S. T. Ro, and W. Wakenham, Physica, 58, No. 2(1965). (1972).
23. O. P. Bahethi, R. S. Gambir, and S. C. Saxena, Z. Naturforsch., 19a, 1478 (1963).
24. A. G. Shashkov and T. N. Abramenko, Thermal Conductivities of Gaseous Mixtures [in Russian], Énergiya, Moscow (1970).

## THERMOPHYSICAL PROPERTIES OF ULTRAFINE BASALT FIBER

V. Ya. Belostotskaya, N. V. Komarovskaya,  
and I. A. Kostyleva

UDC 536.21

An experimental study of the dependence of the thermal conductivity of an ultrafine basalt fiber on the temperature, pressure, and density of the material is reported.

Among modern heat-insulating materials, there is increasing interest in basalt fibers, and the number of articles in which these fibers are used is increasing. Basalt fiber, in addition to having good heat-insulating properties and a good thermal stability, can be obtained from abundant and inexpensive natural resources and, when mass-produced, is relatively inexpensive.

If subjected to vibrations, basalt fiber can be used at temperatures up to 600-650°C over long periods of time; if there is no vibration, the fiber can be used up to 700°C. The thermal stability of basalt fiber can be raised by a one-time stepped heat treatment involving heating of the material to 900°C. The resulting material can be used at temperatures up to 800°C and (briefly) up to 900°C.

Translated from Inzhenerno-Fizicheskii Zhurnal, Vol. 30, No. 4, pp. 680-685, April, 1976. Original article submitted January 27, 1975.

*This material is protected by copyright registered in the name of Plenum Publishing Corporation, 227 West 17th Street, New York, N.Y. 10011. No part of this publication may be reproduced, stored in a retrieval system, or transmitted, in any form or by any means, electronic, mechanical, photocopying, microfilming, recording or otherwise, without written permission of the publisher. A copy of this article is available from the publisher for \$7.50.*